

J.-C. LEE
S. LIM
S.-H. KIM
Y.-H. OH
C.-S. GO[✉]

The filtering characteristics of simple grating optical low-pass filters

Division of Physics and Semiconductor, Wonkwang University, 344-2 Shinyongdong Iksan City, Chonbuk, Korea

Received: 31 October 2001/Revised version: 4 March 2002
Published online: 2 May 2002 • © Springer-Verlag 2002

ABSTRACT We studied the characteristics of a two-dimensional grating optical low-pass filter (GOLF) theoretically and experimentally. The modulation transfer function (MTF) of an optical system that consists of a lens and a GOLF is theoretically derived by taking all orders of diffracted beams into consideration. The MTFs of a two-phase chess-board-type GOLF and a three-phase GOLF were calculated for various phase differences and compared with that of a birefringent low-pass filter (BLF). The three-phase GOLF with nine center beams of equal strength removes most moiré fringes, but the resolution degradation is severe compared to the BLF. The two-phase GOLF with a phase difference of 180° , which is similar to the BLF in term of beam distribution, has a medium characteristic somewhere between those of the three-phase GOLF and the BLF. Samples of two GOLFs are made and experimented on by attaching them to a digital camera. The experimental result coincides with the theoretical development.

PACS 42.30.Kq; 42.30.Lr; 42.79.Dj

1 Introduction

A digital imaging device, such as a charge-coupled device (CCD) or a CMOS image sensor, samples an image by its finite-size image cells. According to the sampling theory, perfect image restoration is possible when the incoming image has spatial frequency components below the Nyquist frequency, which is a half of the inverse value of the sampling period or the pixel size [1, 2]. When the incoming image has a frequency component larger than the Nyquist frequency, image distortion originating from aliasing is inevitable. The moiré fringes that can usually be seen when the image has a fine striped pattern is the best example.

Optical low-pass filters are used in digital imaging systems, such as digital cameras, to filter out high spatial frequency components. The most widely used optical low-pass filter is the birefringent low-pass filter (BLF) that uses polarizing crystal plates to separate incoming light into ordinary and extraordinary beams [3–9]. Since two crystal plates are used to separate incoming light into four beams, a BLF is expensive

as well as thick, which makes it very hard to miniaturize the optical system.

A grating optical low-pass filter (GOLF) is a new alternative to a BLF [10]. Since a thin phase grating on a glass plate is used in a GOLF, it is easy to design optical filters of diverse characteristics by controlling the period and phase differences. And, it can be mass-produced with reasonable tolerance using semiconductor technology. Also, since it is very thin, it can be used in size-sensitive applications. However, the distance between the GOLF and the image sensor must be exact for best performance, and the distance and intensity of the divided light vary according to the wavelength of the incoming light.

By analyzing the one-dimensional modulation transfer function (MTF) of a GOLF, we have reported that a GOLF is optimum when it is used as a nine-beam splitter and the light intensities of the nine beams are the same [11]. We made a GOLF that satisfies this condition by making a three-phase two-dimensional grating on glass. An experimental result by attaching it to a PC camera is also reported. Since high-order diffraction beams (higher than two) are ignored in the one-dimensional model, the diffraction efficiency is less than 80%; hence there is some discrepancy between the one-dimensional model and the measured data.

We calculated a real MTF of a GOLF by considering all higher-order diffraction beams and compared it with that of a BLF. Also, we calculated the MTF of a two-phase chess-board-shaped GOLF to compare with others. We made new samples to verify the analysis. The images through new GOLF samples on digital cameras are compared with those of a BLF.

2 Theory: MTF calculation

The intensity distribution on the image plane can be written as a convolution of the square of the coherent transfer function and the intensity distribution of an object in an incoherent imaging system [12]:

$$I_i(x, y) = |h(x, y)|^2 \times I_o(x, y). \quad (1)$$

For a point source ($I_o(x, y) = \delta(x, y)$),

$$I_i(x, y) = |h(x, y)|^2. \quad (2)$$

✉ Fax: +82-63/858-7389, E-mail: kosoo@wonkwang.ac.kr

By Fourier transforming (2), we can get the optical transfer function (OTF), H , of the imaging system:

$$H(\xi, \eta) = F [|h(x, y)|^2] = F [I_i(x, y)]. \quad (3)$$

Hence, we can calculate the OTF (or MTF) of an imaging system, if we know the image intensity of a point-source object.

Let us consider an incoherent imaging system that consists of a lens system and a GOLF. The wave function on the image plane U_i is proportional to the Fourier transform of the GOLF transmittance subtended by the lens pupil [13]:

$$\begin{aligned} U_i(x, y) &= e^{i\pi(x^2+y^2)/\lambda d} \\ &\times \iint P(\alpha, \beta) t_g(\alpha, \beta) e^{-2\pi i(x\alpha+y\beta)/\lambda d} d\alpha d\beta \\ &\propto F [P t_g] \left(\frac{x}{\lambda d}, \frac{y}{\lambda d} \right) \\ &= (F[P] \times F[t_g]) \left(\frac{x}{\lambda d}, \frac{y}{\lambda d} \right), \end{aligned} \quad (4)$$

where $P(x, y)$ is the lens-pupil function, $t_g(x, y)$ is the GOLF transmittance, λ is the wavelength, and d is the distance from the lens to the image plane. Since the GOLF transmittance is a periodic function, the Fourier transform of it is the sum of delta functions and can be written as follows:

$$F[t_g] \left(\frac{x}{\lambda d}, \frac{y}{\lambda d} \right) = \sum_{m,n} a_{m,n} \delta(x - mx_0) \delta(y - ny_0), \quad (5)$$

where $x_0 = \lambda d/p_x$, $y_0 = \lambda d/p_y$, and p_x and p_y are the periods of the GOLF in the x and y directions, respectively. The coefficient $a_{m,n}$ depends on the structure of the GOLF. From (4) and (5),

$$U_i(x, y) = e^{i\pi(x^2+y^2)/\lambda d} \sum_{m,n} a_{m,n} F[P] \left(\frac{x - mx_0}{\lambda d}, \frac{y - ny_0}{\lambda d} \right) \quad (6)$$

and the image-intensity distribution is

$$I_i(x, y) = \left| \sum_{m,n} a_{m,n} F[P] \left(\frac{x - mx_0}{\lambda d}, \frac{y - ny_0}{\lambda d} \right) \right|^2. \quad (7)$$

When the pupil is a circle of diameter D , the radial extent of $F[P](x/\lambda d, y/\lambda d)$ is about $\lambda d/D$ and is much smaller than x_0 and y_0 . Therefore, we can neglect the overlapping of the terms with different orders (m, n) in (7):

$$I_i(x, y) = \sum_{m,n} \left| a_{m,n} F[P] \left(\frac{x - mx_0}{\lambda d}, \frac{y - ny_0}{\lambda d} \right) \right|^2. \quad (8)$$

Using (3), we can get the OTF of the system:

$$\begin{aligned} H(\xi, \eta) &= F [I_i(x, y)] \\ &= \sum_{m,n} |a_{m,n}|^2 e^{-2\pi i(mx_0\xi + ny_0\eta)} P(\lambda d\xi, \lambda d\eta) \\ &\quad \bullet P^*(\lambda d\xi, \lambda d\eta), \end{aligned} \quad (9)$$

where \bullet means the correlation operation.

For a circular lens of diameter D , the autocorrelation of the pupil function becomes [14]:

$$\begin{aligned} P(\lambda d\xi, \lambda d\eta) \bullet P^*(\lambda d\xi, \lambda d\eta) &= \\ \frac{2}{\pi} &\left[\cos^{-1} \frac{\sqrt{\xi^2 + \eta^2}}{f_{\max}} - \frac{\sqrt{\xi^2 + \eta^2}}{f_{\max}} \sqrt{1 - \frac{\xi^2 + \eta^2}{f_{\max}^2}} \right] \\ &\text{if } \sqrt{\xi^2 + \eta^2} \leq f_{\max}, 0, \text{ otherwise,} \end{aligned} \quad (10)$$

where $f_{\max} = D/\lambda d = 2NA/\lambda$.

2.1 MTF of two-phase GOLF

The phase structure of a two-phase GOLF is shown in Fig. 1a. By Fourier transforming the GOLF transmittance, we can get the coefficient $a_{m,n}$ as follows:

$$\begin{aligned} a_{m,n} &= \frac{2 \sin(m\pi/2) \sin(n\pi/2)}{mn\pi^2} \\ &\times \left[\cos \frac{m+n}{2} \pi + e^{i\phi} \cos \frac{m-n}{2} \pi \right], \end{aligned} \quad (11)$$

where ϕ is the phase difference of the GOLF. Except for $a_{0,0}$, $a_{m,n}$ is zero if m or n is even. Using the symmetry $|a_{m,n}|^2 = |a_{m,-n}|^2 = |a_{-m,n}|^2 = |a_{-m,-n}|^2$, the OTF becomes:

$$\begin{aligned} H(\xi, \eta) &= P(\lambda d\xi, \lambda d\eta) \bullet P^*(\lambda d\xi, \lambda d\eta) \\ &\times \left\{ |a_{0,0}|^2 + 4 \sum_{m,n=1}^{\infty} |a_{2m-1, 2n-1}|^2 \right. \\ &\quad \left. \times \cos [2\pi(2m-1)x_0\xi] \cos [2\pi(2n-1)y_0\eta] \right\}. \end{aligned} \quad (12)$$

0	ϕ	0	ϕ
ϕ	0	ϕ	0
0	ϕ	0	ϕ
ϕ	0	ϕ	0

0	ϕ	0	ϕ
ϕ	2ϕ	ϕ	2ϕ
0	ϕ	0	ϕ
ϕ	2ϕ	ϕ	2ϕ

a

b

FIGURE 1 The phase structure of a GOLF. **a** Two-phase GOLF, **b** three-phase GOLF

2.2 MTF of three-phase GOLF

The phase structure of a three-phase GOLF is shown in Fig. 1b. The coefficient $a_{m,n}$ becomes:

$$\begin{aligned} a_{m,n} &= \frac{2 \sin(m\pi/2) \sin(n\pi/2)}{mn\pi^2} \\ &\times \left[\cos \frac{m+n}{2} \pi + \cos \left(\frac{m-n}{2} \pi - \phi \right) \right]. \end{aligned} \quad (13)$$

The symmetry $|a_{m,n}|^2 = |a_{m,-n}|^2 = |a_{-m,n}|^2 = |a_{-m,-n}|^2$ is also preserved, but $|a_{m,0}|^2 = |a_{0,m}|^2 \neq 0$ in this case. Hence

$$\begin{aligned}
 H(\xi, \eta) = & P(\lambda d\xi, \lambda d\eta) \bullet P^*(\lambda d\xi, \lambda d\eta) \left\{ |a_{0,0}|^2 \right. \\
 & + 2 \sum_{m=1}^{\infty} |a_{2m-1,0}|^2 \\
 & \quad \times (\cos [2\pi(2m-1)x_0\xi] + \cos [2\pi(2m-1)y_0\eta]) \\
 & + 4 \sum_{m,n=1}^{\infty} |a_{2m-1,2n-1}|^2 \cos [2\pi(2m-1)x_0\xi] \\
 & \quad \left. \times \cos [2\pi(2n-1)y_0\eta] \right\} \quad (14)
 \end{aligned}$$

2.3 MTF of BLF

A BLF is a four-beam splitter and has no higher orders. The only nonzero terms are $|a_{1,1}|^2 = |a_{1,-1}|^2 = |a_{-1,1}|^2 = |a_{-1,-1}|^2 = 0.25$. Hence

$$\begin{aligned}
 H(\xi, \eta) = & P(\lambda d\xi, \lambda d\eta) \\
 & \bullet P^*(\lambda d\xi, \lambda d\eta) \cos[2\pi x_0\xi] \cos[2\pi y_0\eta]. \quad (15)
 \end{aligned}$$

3 MTF analysis

An ideal filter is one that cuts out all spatial frequency components above the Nyquist frequency, f_N , and passes all components below f_N . If the MTF value below f_N is small, the resolution of an imaging system deteriorates. If the MTF value above f_N is large, severe moiré fringes may occur. Therefore, we can estimate the performance of three filters by comparing their MTFs.

In a two-phase GOLF, if the phase difference is π , the 0th-order beam disappears and four beams of ± 1 st order are the strongest; thus it shows a characteristic similar to that of a BLF. As the phase difference becomes smaller, the intensity of the 0th-order beam at the center increases. In this case, a GOLF works as a five-beam splitter. We can conclude that the less the phase difference, the better the resolution of the imaging system and the less the filtering effect. The MTF of a GOLF with several phase differences is shown in Fig. 2a. The MTF of a BLF is also shown. The graph is the cross-sectional view at the ξ -axis ($\eta = 0$) from the (ξ, η) plane. For the graph, diffraction beams up to the ± 100 th orders in the x and y directions are taken into consideration. The x_0 value in (12) is half of the pixel size and the spatial frequency is normalized by f_N . For most spatial frequencies, the MTF value of a GOLF is less than that of a BLF if the phase difference is π . Therefore, we may conclude that an imaging system with a GOLF shows more resolution degradation than that with a BLF, while it has better moiré filtering.

If the phase difference is less than π , we can see that the MTF values at frequencies lower than f_N are obviously improved, but there is no specific tendency at frequencies higher than f_N . In the case $\phi = 100^\circ$, the resolution is better than

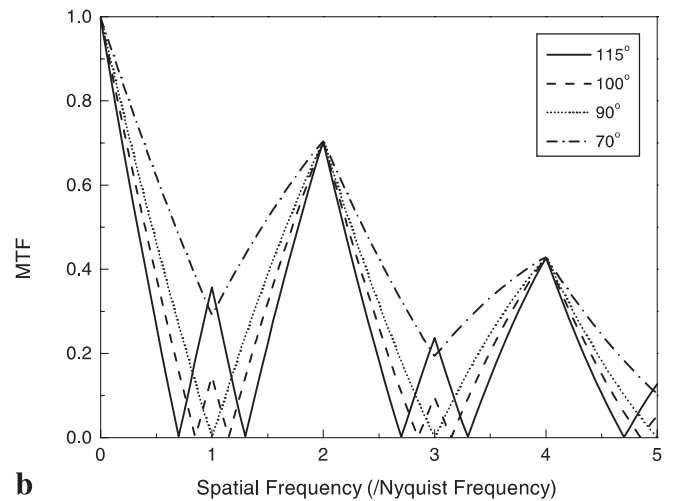
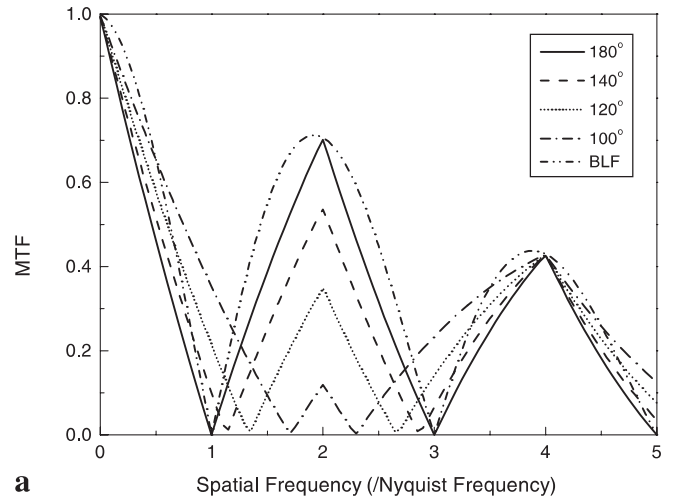


FIGURE 2 The MTF of a two-phase GOLF (a) and a three-phase GOLF (b). The numbers in the boxes are the phase differences (ϕ) of the GOLF. The MTF of a BLF is also shown in (a)

that of a BLF and the filtering characteristic at frequencies between $1.2 f_N$ and $2.8 f_N$ is much better than that of a BLF. But, higher-frequency components may degrade the moiré fringe.

In the case of a three-phase GOLF in Fig. 1b, if the phase $\phi = 115^\circ$, the intensities of nine beams at the center are all same. But, if the phase is less than this value, the resolution is improved while the filtering effect is degraded, since the 0th-order beam at the center becomes stronger. The MTF of the three-phase GOLF is shown in Fig. 2b. In this case, most of the conditions are the same as those of the two-phase GOLF, but the x_0 value is the pixel size. When $\phi = 115^\circ$, the resolution is less than that of a two-phase GOLF with phase π , but the filtering effect is better. As the phase difference decreases, the resolution improves, while the filtering deteriorates. One should note that the MTF of the three-phase GOLF with $\phi = 1/2\pi(90^\circ)$ is almost same as that of a two-phase GOLF with $\phi = \pi(180^\circ)$.

In the two types of GOLF, the resolution improves while the filtering effect degrades, as the phase difference decreases. But, the filtering effect degradation of the three-phase GOLF in Fig. 2b is too severe. Therefore, the two-phase GOLF is recommended for better resolution with tolerable moiré fringes.

4 Experiments and results

We manufactured two types of GOLF samples shown in Fig. 1. The two-dimensional phase gratings are made by etching soda lime silica glass plates with a thickness of 1 mm through a semiconductor lithography process. Since the refractive index of the glass is 1.523 and the reference wavelength of visible light is 550 nm (green), the etch depth of a phase difference π is 530 nm. We fabricated a two-phase GOLF with $\phi = 180^\circ$ and a three-phase GOLF with $\phi = 115^\circ$. The process margin of the etch depth was ± 10 nm and the corresponding error bound in the phase difference is $\pm 3.4^\circ$. This value has little effect on the filtering characteristics of a GOLF, as we can see in Fig. 2. The period of a three-phase GOLF was $330 \mu\text{m}$ and that of a two-phase GOLF was $660 \mu\text{m}$. The error in the width of each phase step is of the order of the etch depth and hence can be ignored.

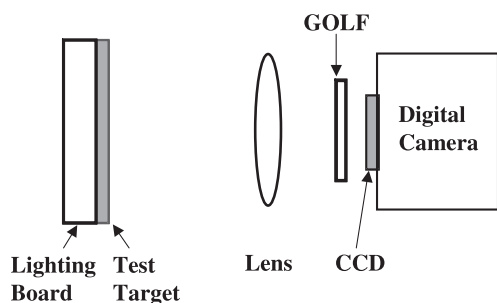


FIGURE 3 The experimental setup

The experimental setting is shown in Fig. 3. The imaging device is a digital camera from Samsung Electronics (model SDC007). For reference, the CCD in the camera is a Matsushita MN3778, which has 1152×872 effective pixels, the size of each pixel being $4.6 \mu\text{m} \times 4.6 \mu\text{m}$. The original camera lens was replaced with a Pentax lens with a larger focal length. A GOLF or a BLF was placed between the lens and the CCD to take a picture of test targets. All optical devices including the lens and the GOLF were placed on micro-translators to adjust their positions. The F# of the lens is fixed to 2.8. A zone-plate image was used to observe the moiré fringes and a USAF1951 resolution chart was used to measure the resolution. The effective distance from the CCD surface to the GOLF is 2.8 mm and the distance from the glass lid to the GOLF is 1.3 mm.

Zone-plate images of four cases are shown in Fig. 4. We compared images without any optical filter, with a BLF, and two kinds of GOLF, a two-phase GOLF with $\phi = 180^\circ$ and a three-phase GOLF with $\phi = 115^\circ$. To make the difference in the filtering effect more distinctive, we used a graphic program to filter each picture. In all images, concentric circles are all moiré fringes if the center of the circle is not at the center of the image. We can conclude that the moiré fringes are remarkably reduced if any kind of filter is used. The moiré fringes with a BLF were the most severe. The two types of GOLF show similar moiré reduction, but the three-phase GOLF with $\phi = 115^\circ$ in Fig. 4c shows the fewest moiré fringes. The experimental results match the conclusions we obtained from the MTF comparison in Fig. 2.

Images of the resolution chart are shown in Fig. 5. The image is the clearest of all without any filter in Fig. 5a.

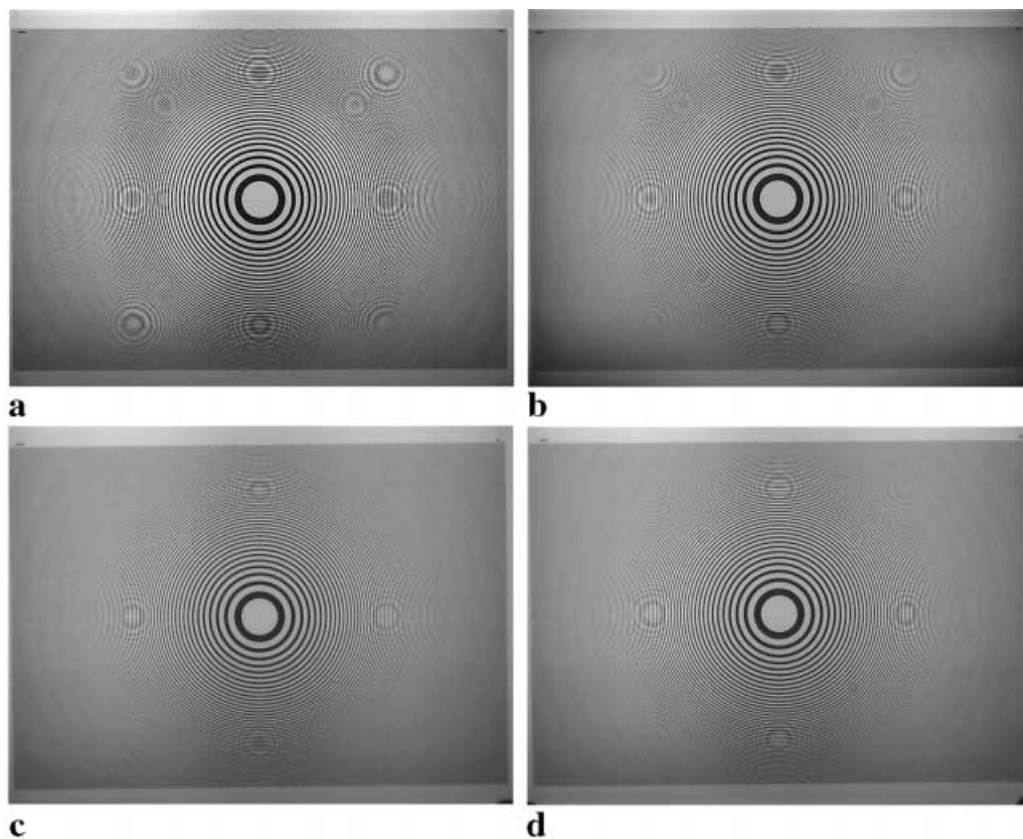


FIGURE 4 The images of a zone plate. To make them more distinctive, we filtered all the figures with the same graphic operation (using Adobe Photoshop). **a** Without any filter, **b** with BLF, **c** with three-phase GOLF ($\phi = 115^\circ$), and **d** with two-phase GOLF ($\phi = 180^\circ$)

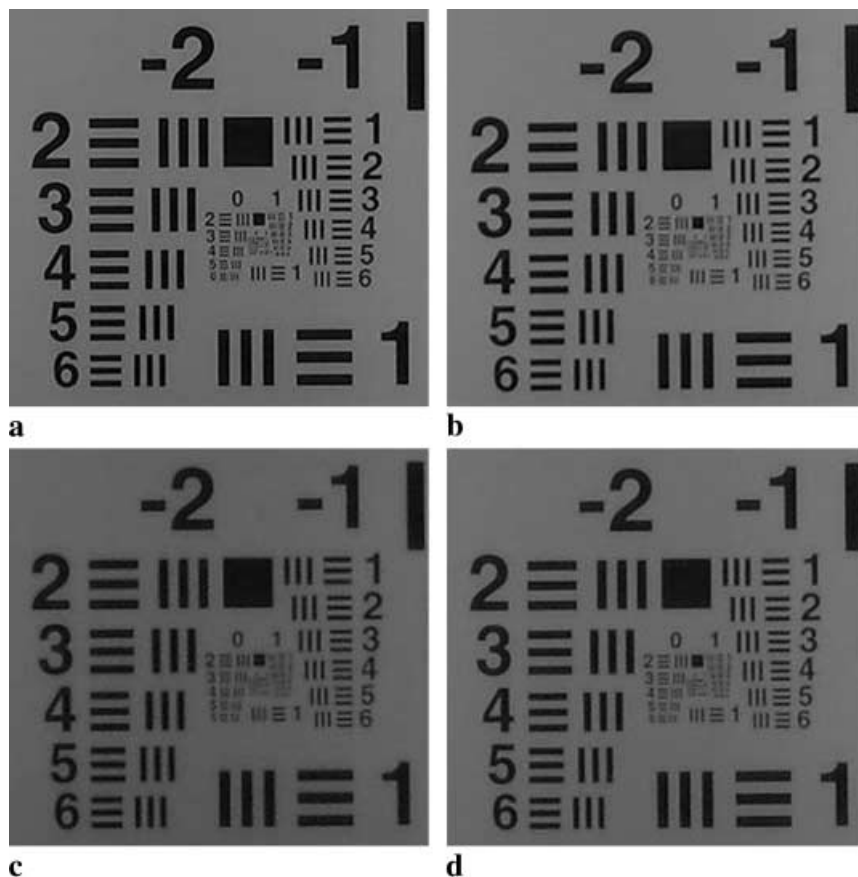


FIGURE 5 The images of a USAF resolution chart. **a** Without any filter, **b** with BLF, **c** with three-phase GOLF ($\phi = 115^\circ$), and **d** with two-phase GOLF ($\phi = 180^\circ$)

The image with a BLF is the next (Fig. 5b), and the image with a three-phase GOLF ($\phi = 115^\circ$) shows the least clarity (Fig. 5c). For example, if we calculate the maximum modulation of the horizontal lines in element 2 of group 0, it is 0.86 without an optical filter, 0.43 with a BLF, 0.16 with a three-phase GOLF ($\phi = 115^\circ$), and 0.30 with a two-phase GOLF ($\phi = 180^\circ$), which coincides with the sequence we predicted from the theory.

5 Summary and future work

The theoretical MTF of a GOLF was derived by taking all diffraction beams of high orders into consideration. The MTF of a two-phase chess-board-type GOLF and that of a three-phase GOLF were analyzed and compared with that of a BLF. The GOLF was manufactured with a semiconductor process and attached to a digital camera. Images of a test target were taken with and without optical filters and compared in terms of resolution and filtering effect.

As the phase difference of the GOLF increases, the filtering effect improves, and thus fewer moiré fringes are shown, but the resolution degrades. The resolution of the BLF was the best in all tested optical filters, but the filtering effect was the worst and the most moiré fringes were visible. The three-phase GOLF with $\phi = 115^\circ$, which has nine beams with equal strength, shows the best filtering effect and the worst resolution. The two-phase GOLF with $\phi = 180^\circ$ shows characteristics somewhere between the two. This experimental result agrees with the theoretical prediction from the MTF.

In this experiment, we found that the grating image is superimposed on object images in special conditions. Vague lines visible in the outer part of the image in Fig. 4c and d are grating lines of the x or y direction. This is the Fresnel image and it is more distinctive when the F# of the lens increases. We are working to solve the problem.

ACKNOWLEDGEMENTS This work was supported by the Wonkwang University in 2000. The GOLF samples were made by the Havit Information Co. of Korea.

REFERENCES

- 1 J.D. Gaskill: *Linear Systems, Fourier Transforms, and Optics* (Wiley, New York 1978) pp. 266–285
- 2 J.W. Goodman: *Introduction to Fourier Optics* (McGraw-Hill, New York 1968) pp. 21–25
- 3 A. Nordbryhn: Proc. SPIE **476**, 116 (1983)
- 4 O. Yoshida, S. Tagawa, M. Achiba: J. Inst. Telev. Eng. Jpn. **38**, 249 (1984)
- 5 O. Yoshida, A. Iwamoto: J. Inst. Telev. Eng. Jpn. **38**, 745 (1984)
- 6 Y. Ohtake: US Patent No. 4 539 584 (1985)
- 7 M. Sato, S. Nagahara, K. Takahashi: US Patent No. 4 626 897 (1986)
- 8 T. Asaida: US Patent No. 4 761 682 (1988)
- 9 J.E. Greivenkamp: Appl. Opt. **29**, 676 (1990)
- 10 K. Fuisawa, M. Uetsiki, Y. Nishida: Jpn. J. Appl. Phys. **35**, 1768 (1996)
- 11 C.-S. Go, S. Lim, S. Kim, J.-C. Lee, Y.-H. Oh: Appl. Phys. B **73**, 721 (2001)
- 12 J.W. Goodman: *Introduction to Fourier Optics* (McGraw-Hill, New York 1968) p. 121
- 13 J.W. Goodman: *Introduction to Fourier Optics* (McGraw-Hill, New York 1968) pp. 88–90
- 14 J.W. Goodman: *Introduction to Fourier Optics* (McGraw-Hill, New York 1968) pp. 119–120